An Update of the Quasi-Analytical Algorithm (QAA_v5)

ZhongPing Lee[1], Bertrand Lubac[1], Jeremy Werdell[2], Robert Arnone[3]

[1]Northern Gulf Institute, Mississippi State University
Stennis Space Center, MS 39529
zplee@ngi.msstate.edu

[2]Ocean Biology Processing Group, GSFC, NASA

[3]Naval Research Laboratory, Stennis Space Center

Table 1. A contrast between QAA_v4 and QAA_v5

	$r_{rs}(\lambda) = R_{rs}(\lambda)/(0.52 + 1.7\,R_{rs}(\lambda))$	
$u = b_b/(a+b_b)$	$r_{rs}(\lambda) = (g_0 + g_1 u(\lambda))u(\lambda)$ $u(\lambda) = \frac{-g_0 + \sqrt{(g_0)^2 + 4g_1 * r_{rs}(\lambda)}}{2g_1}$; g_0=0.089,g_1=0.125	
	QAA_v5	**QAA_v4**
λ_0 = 550; 555; 560	$\chi = \log\left(\frac{r_{rs}(443)+r_{rs}(490)}{r_{rs}(\lambda_0)+5\frac{r_{rs}(667)}{r_{rs}(490)}r_{rs}(667)}\right)$, $a(\lambda_0) = a_w(\lambda_0) + 10^{-1.146-1.366\chi-0.469\chi^2}$	$\chi = \log\left(\frac{r_{rs}(443)+r_{rs}(490)}{r_{rs}(\lambda_0)+2\frac{r_{rs}(640)}{r_{rs}(490)}r_{rs}(640)}\right)$, $a(\lambda_0) = a_w(\lambda_0) + 10^{h0+h1\chi+h2\chi^2}$
Exponent of $b_{bp}(\lambda)$	$\eta = 2.0\left(1-1.2\,\exp\left(-0.9\frac{r_{rs}(443)}{r_{rs}(\lambda_0)}\right)\right)$	$\eta = 2.2\left(1-1.2\,\exp\left(-0.9\frac{r_{rs}(443)}{r_{rs}(555)}\right)\right)$
ζ: $a_{ph}411/a_{ph}443$	$\zeta = 0.74 + \frac{0.2}{0.8 + r_{rs}(443)/r_{rs}(\lambda_0)}$	$\zeta = 0.71 + \frac{0.06}{0.8 + r_{rs}(443)/r_{rs}(555)}$
ξ: $a_{dg}411/a_{dg}443$	$\xi = e^{S(443-411)}$, $S = 0.015 + \frac{0.002}{0.6 + r_{rs}(443)/r_{rs}(\lambda_0)}$	$\xi = e^{S(443-411)}$, $S = 0.015$
Upper limit for $R_{rs}(667)$	$R_{rs}(667) = 20.0(R_{rs}(\lambda_0))^{1.5}$	$R_{rs}(640) = 0.01R_{rs}(555) + 1.4R_{rs}(667) - 0.0005\frac{R_{rs}(667)}{R_{rs}(490)}$
Lower limit for $R_{rs}(667)$	$R_{rs}(667) = 0.9(R_{rs}(\lambda_0))^{1.7}$	
If no $R_{rs}(667)$ measurements or measured $R_{rs}(667)$ out of the limits	$R_{rs}(667) = 1.27(R_{rs}(\lambda_0))^{1.47} + 0.00018\left(\frac{R_{rs}(490)}{R_{rs}(\lambda_0)}\right)^{3.19}$	

Descriptions

The Quasi-Analytical Algorithm (QAA) was originally developed by *Lee et al.* [2002] to derive the absorption and backscattering coefficients by analytically inverting the spectral remote-sensing reflectance ($R_{rs}(\lambda)$). QAA starts with the calculation of the

total absorption coefficient (a) at a reference wavelength (λ_0), and then propagate the calculation to other wavelengths. Component absorption coefficients (contributions by detritus/gelbstoff and phytoplankton pigments) are further algebraically decomposed from the total absorption spectrum. To summarize, briefly, QAA is consist of the following elements:

1) The ratio of backscattering coefficient (b_b) to the sum of backscattering and absorption coefficients ($b_b/(a+b_b)$) at λ is calculated algebraically based on the models of *Gordon et al*. [1988] and *Lee et al*. [1999],

$$\frac{b_b(\lambda)}{a(\lambda)+b_b(\lambda)} = \frac{-0.0895+\sqrt{0.008+0.499\,r_{rs}(\lambda)}}{0.249}. \quad (1)$$

Here $r_{rs}(\lambda)$ is the nadir-viewing spectral remote-sensing reflectance just below the surface and is calculated from nadir-viewing $R_{rs}(\lambda)$ through,

$$r_{rs}(\lambda) = R_{rs}(\lambda)/(0.52 + 1.7\,R_{rs}(\lambda)). \quad (2)$$

2) The spectral $b_b(\lambda)$ is modeled with the widely used expression [*Gordon and Morel*, 1983; *Smith and Baker*, 1981],

$$b_b(\lambda) = b_{bw}(\lambda) + b_{bp}(\lambda_0)\left(\frac{\lambda_0}{\lambda}\right)^{\eta}, \quad (3)$$

where b_{bw} and b_{bp} are the backscattering coefficients of pure seawater and suspended particles, respectively. Values of $b_{bw}(\lambda)$ are provided in *Morel* [1974].

3) When $a(\lambda_0)$, the ratio of $b_b/(a+b_b)$ at λ_0, and $b_{bw}(\lambda_0)$ are known, $b_{bp}(\lambda_0)$ in Eq. 3 can be easily derived with the combination of Eqs. 1 and 3. The values of $b_b(\lambda)$ at other wavelengths are then calculated after the power parameter (η) is estimated [*Lee et al.*, 2002].

4) Applying $b_b(\lambda)$ to the ratio of $b_b/(a+b_b)$ at λ (Eq. 1), the total absorption coefficient at λ, $a(\lambda)$, is then calculated algebraically.

5) After $a(\lambda)$ is known, $a_{dg}(\lambda)$ and $a_{ph}(\lambda)$ is calculated through

$$\begin{cases} a_{dg}(443) = \dfrac{\left(a(411)-\zeta\, a(443)\right)-\left(a_w(411)-\zeta\, a_w(443)\right)}{\xi-\zeta}, \\ a_{ph}(\lambda) = a(\lambda) - a_w(\lambda) - a_{dg}(443)e^{-S(\lambda-443)}. \end{cases} \quad (4)$$

Here $\zeta = a_{ph}(411)/a_{ph}(443)$ and $\xi = a_{dg}(411)/a_{dg}(443)$.

The updates of the QAA (related to the calculation of $a(\lambda_0)$, η, ζ, and ξ)

In QAA_v4 [*Lee et al.*, 2007] an estimated $R_{rs}(640)$ was proposed for the calculation of $a(\lambda_0)$ for both oceanic and coastal waters. Recent studies have found that this empirical estimation is not that robust. To overcome this short come, the measured $R_{rs}(667)$ (or a wavelength in the near vicinity) is now incorporated directly. This is in particular useful because that all operational satellite sensors (SeaWiFS, MODIS, and MERIS) have a band at this wavelength, although some minor contamination from chlorophyll fluorescence is possible in the measured $R_{rs}(667)$.

Therefore, in this updated version of QAA (v5), $a(\lambda_0)$ is now estimated as follow,

$$\begin{cases} \chi = \log\left(\dfrac{r_{rs}(443) + r_{rs}(490)}{r_{rs}(\lambda_0) + 5\dfrac{r_{rs}(667)}{r_{rs}(490)} r_{rs}(667)} \right), & (5) \\ a(\lambda_0) = a_w(\lambda_0) + 10^{-1.146 - 1.366\chi - 0.469\chi^2}, & (6) \end{cases}$$

with λ_0 as 550, 555, or 560 nm that corresponding to SeaWiFS, MODIS, and MERIS sensors.

Constants in Eq. 6 were the average of the coefficients obtained by least-square fitting $a(\lambda_0)$ of the synthetic data set adopted by the IOCCG [2006] for SeaWiFS, MODIS, and MERIS bands. In short, one set of parameters is proposed for the three sensors (good enough for comparison of derived IOPs with in situ measurements), except the change of $a_w(\lambda_0)$ values for each sensor. Separate sets of constants for each sensor, however, are necessary if long-term and consistent IOP results from the three sensors are the goal.

When processing data from satellite imageries, $R_{rs}(667)$ could be erroneous due to imperfect atmospheric correction. Consequently, constraints for the $R_{rs}(667)$ value are necessary in order to avoid the impact of erroneous $R_{rs}(667)$ on IOPs at the shorter wavelengths. Based on *in situ* measurements and Hydrolight simulated data, Figure 1a shows the range of $R_{rs}(667)$ for the different $R_{rs}(555)$, along with the upper and lower bands: For each $R_{rs}(555)$, $R_{rs}(667)$ is proposed to be kept within

Upper limit:

$$R_{rs}(667) = 20.0\left(R_{rs}(555)\right)^{1.5}. \quad (7)$$

Lower limit

$$R_{rs}(667) = 0.9\left(R_{rs}(555)\right)^{1.7}. \quad (8)$$

If there is no $R_{rs}(667)$ measurement or $R_{rs}(667)$ value is out of the limits, an estimated $R_{rs}(667)$ is provided, i.e.

$$R_{rs}(667) = 1.27\left(R_{rs}(555)\right)^{1.47} + 0.00018\left(R_{rs}(490/R_{rs}(555)\right)^{-3.19}, \quad (9)$$

Which is the best regression (Figure 1b) between $R_{rs}(667)$ and $R_{rs}(555)$ as well as $R_{rs}(490)/R_{rs}(555)$.

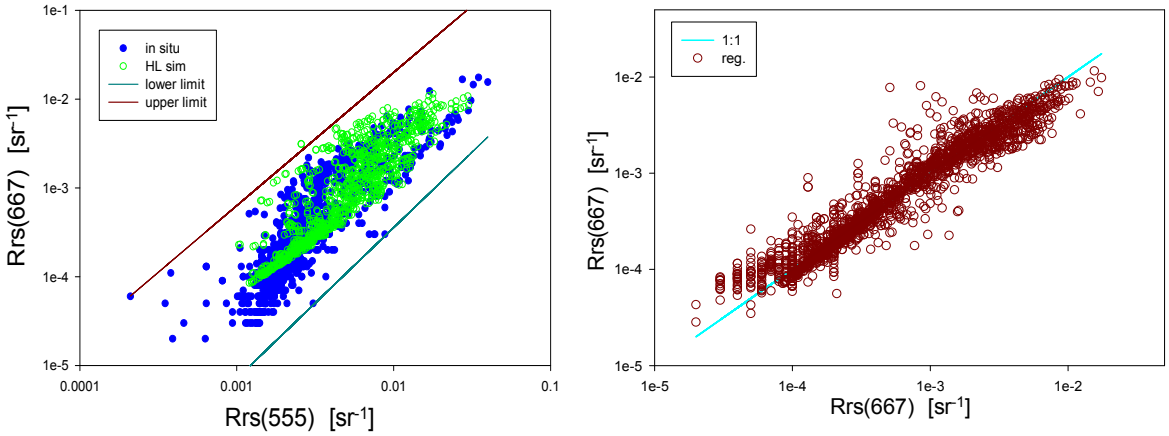

Figure 1a (left), upper and lower limits of $R_{rs}(667)$. 1b (right): empirical $R_{rs}(667)$ from $R_{rs}(555)$ and $R_{rs}(490)/R_{rs}(555)$.

Value of η, required for extrapolation of b_{bp} at λ_0 to shorter wavelengths, is now slightly adjusted to the following based on NOMAD dataset (see Fig.2)

$$\eta = 2.0\left(1 - 1.2\ \exp\left(-0.9\frac{r_{rs}(443)}{r_{rs}(555)}\right)\right). \quad (10)$$

The 555 nm used in Eqs. 7-10 can be changed to 550 nm (for MODIS) or 560 nm (for MERIS) without causing significant impacts on final IOP results.

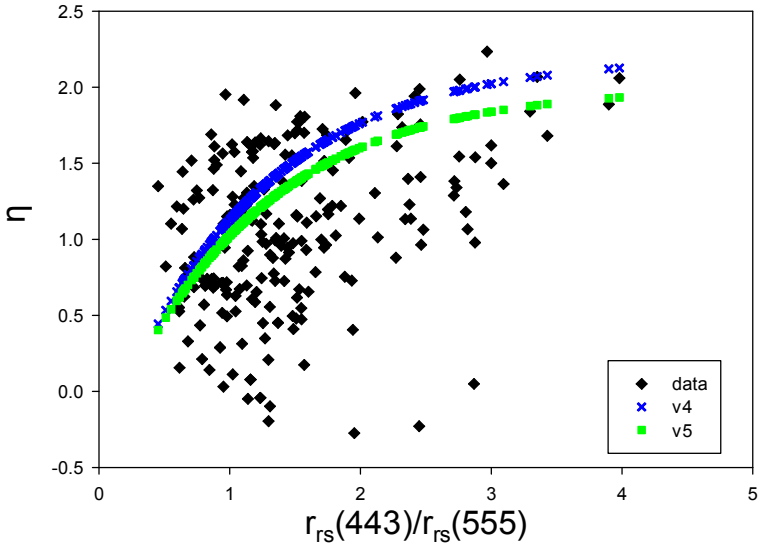

Figure 2. Relationship between η (Y-axis) and $r_{rs}(443)/r_{rs}(555)$ (X-axis). Symbol square for data, blue line for Eq.10, green line for estimates by QAA-v4.

Values of ζ (= $a_{ph}411/a_{ph}443$), and ξ (= $a_{dg}411/a_{dg}443$) are required for the analytical decomposition of the total absorption spectrum, and their estimations are adjusted to the following, respectively (Fig.3)

$$\zeta = 0.74 + \frac{0.2}{0.8 + r_{rs}(443)/r_{rs}(555)} \tag{11}$$

$$\xi = e^{S(443-411)}, \quad S = 0.015 + \frac{0.002}{0.6 + r_{rs}(443)/r_{rs}(555)} \tag{12}$$

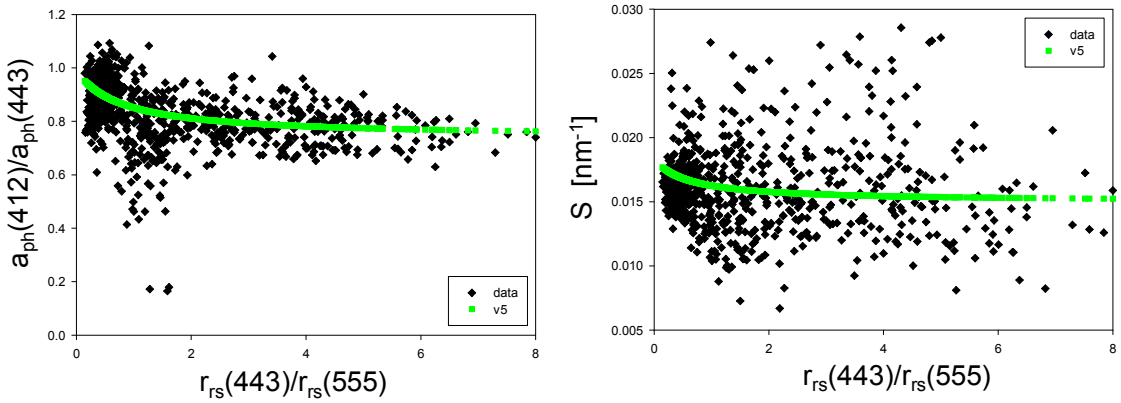

Figure 3. Relationships between $a_{ph}(411)/a_{ph}(443)$ (left), S (right), and $r_{rs}(443)/r_{rs}(555)$ (X-axis), respectively. Data points with $a_{ph}(411)/a_{ph}(443) > 1.1$ are excluded.

Evaluation

The above updated parameterization (QAA_v5) is applied to the latest NOMAD dataset, and it is found that inverted results are quite consistent with *in situ* values for wide range of waters (Fig. 4). Note that there is no screening of the measurements, and all retrievals are included except negative values (5% for $a_{ph}443$, and 1% for $a_{dg}443$). Systematically higher estimation of b_{bp} is found when compared to *in situ* measurements, where more analyses are needed to understand the differences. $K_d(490)$ is calculated further with QAA derived $a(490)$ and $b_b(490)$ based on the model of Lee et al [2005]. Comparing to the results from QAA_v4, higher absorption and backscattering coefficients are derived for waters with $a(443) > 0.5$ m^{-1} (see Fig. 5), with significantly better retrievals are found for $a_{ph}(443)$. Statistical analysis (in Log scale) of QAA-v4 and QAA_v5 retrieved properties are provided in Table 2, where RMS represents root-mean-square difference (in Log scale) between retrieved and measured property.

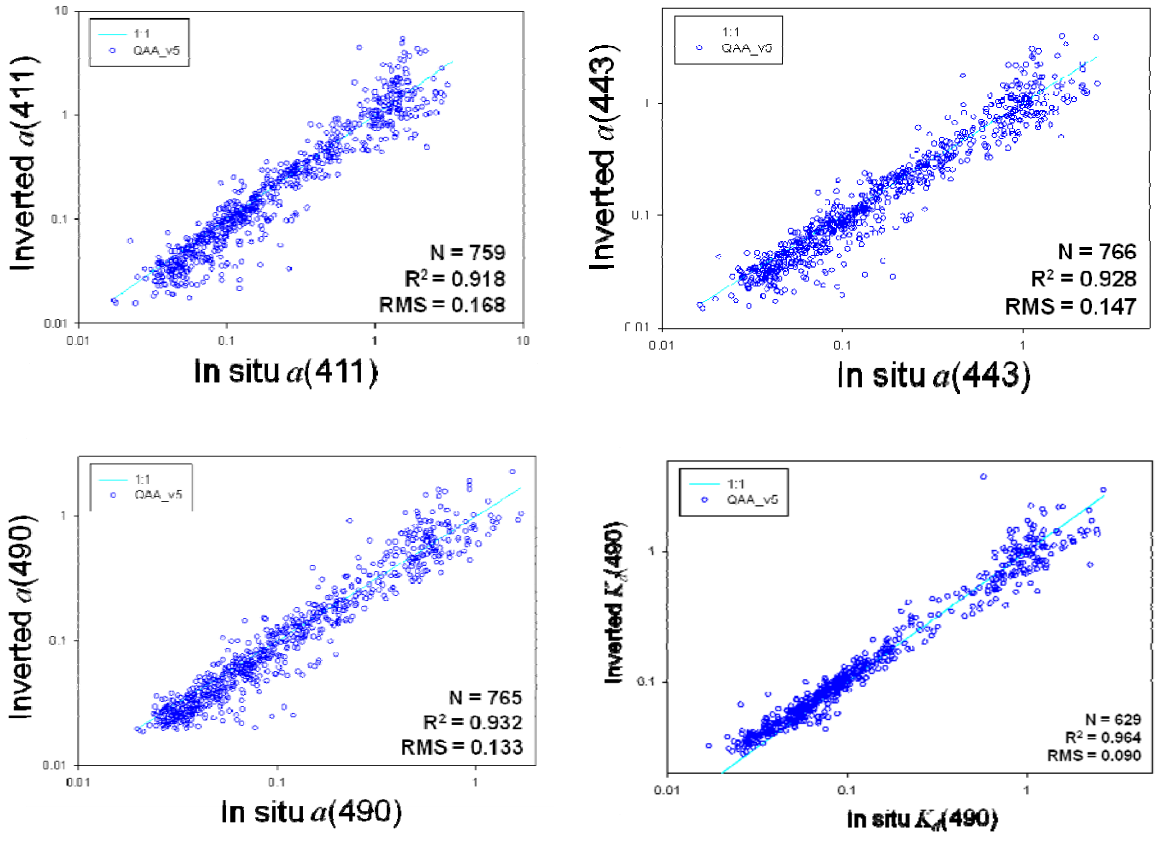

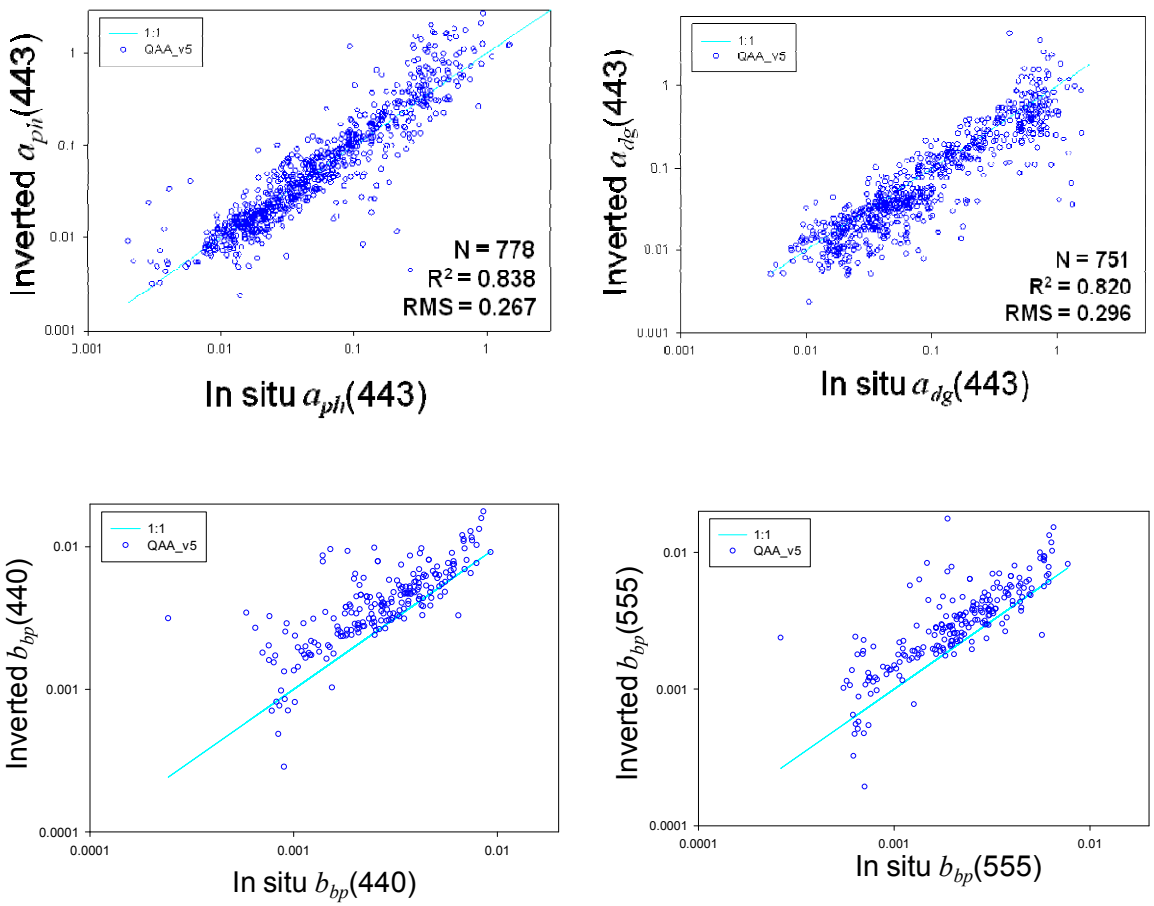

Figure 4. Performance of QAA-v5 with NOMAD data set.

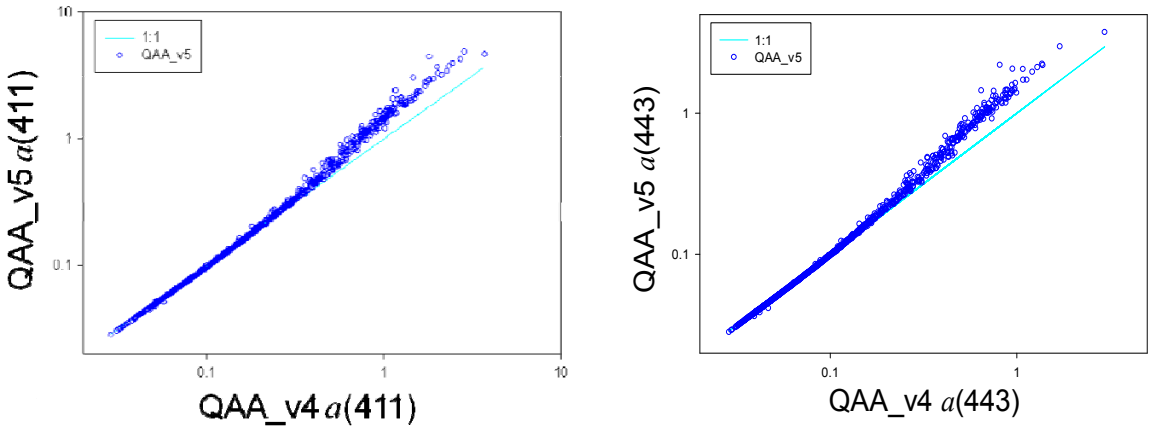

Figure 5. Results of QAA-v5 versus that of QAA-v4 when applied to NOMAD data set.

Table 2: Summary of QAA performance (NOMAD)

	QAA_v4		QAA_v5	
	R^2	RMS	R^2	RMS
$a(411)$	0.902	0.202	0.918	0.168
$a(443)$	0.918	0.185	0.928	0.147
$a(490)$	0.925	0.159	0.932	0.133
$K_d(490)$	0.959	0.146	0.964	0.090
$a_{ph}(443)$	0.675	0.405	0.838	0.267
$a_{dg}(443)$	0.820	0.238	0.820	0.296

Reference:

Gordon, H. R., and A. Morel (1983), *Remote assessment of ocean color for interpretation of satellite visible imagery: A review*, 44 pp., Springer-Verlag, New York.

Gordon, H. R., et al. (1988), A semianalytic radiance model of ocean color, *J. Geophys. Res.*, *93*, 10,909-910,924.

IOCCG (2006), Remote Sensing of Inherent Optical Properties: Fundamentals, Tests of Algorithms, and Applications, in *Reports of the International Ocean-Colour Coordinating Group, No. 5*, edited by Z.-P. Lee, p. 126, IOCCG, Dartmouth, Canada.

Lee, Z. P., et al. (1999), Hyperspectral remote sensing for shallow waters: 2. Deriving bottom depths and water properties by optimization, *Applied Optics*, *38*, 3831-3843.

Lee, Z. P., et al. (2002), Deriving inherent optical properties from water color: A multi-band quasi-analytical algorithm for optically deep waters, *Applied Optics*, *41*, 5755-5772.

Lee, Z. P., et al. (2005), Diffuse attenuation coefficient of downwelling irradiance: An evaluation of remote sensing methods, *J. Geophys. Res.*, *110*(C02017), doi:10.1029/2004JC002573.

Lee, Z. P., et al. (2007), Euphotic zone depth: Its derivation and implication to ocean-color remote sensing, *J. Geophys. Res.*, *112*, C03009, doi:03010.01029/02006JC003802.

Morel, A. (1974), Optical properties of pure water and pure sea water, in *Optical Aspects of Oceanography*, edited by N. G. Jerlov, and Nielsen, E. S., pp. 1-24, Academic, New York.

Smith, R. C., and K. S. Baker (1981), Optical properties of the clearest natural waters, *Applied Optics*, *20*, 177-184.